



Assessment of deflection-based and seismic non-destructive methods to identify delamination of HMA pavements

F. Selcan Ozen^{a,*}, Manuel Celaya^b, Soheil Nazarian^c, Mehmet Saltan^d

^aMinistry of Transport, Maritime Affairs and Communications, Ankara, Turkey

^bAdvanced Infrastructure Design, Inc., Hamilton, NJ, USA

^cDepartment of Civil Engineering, University of Texas at El Paso, El Paso, TX, USA

^dCivil Engineering Department, Engineering Faculty, Suleyman Demirel University, Turkey

Highlights

- USW and FWD are capable to locate damaged areas
- USW detect 53% of the debonded areas
- FWD detect 46% of the debonded areas

Abstract

Timely and cost effective maintenance activities are required to perform well under changing climatic conditions during service life of a hot mix asphalt (HMA) pavement. Pavement maintenance and rehabilitation process plays an important role for cost-effective pavement life cycle. Nondestructive testing methods provide to getting significant and rapidly information about the pavement without causing any damage on the surface of the pavement. In this paper, for early detection of delamination of asphalt surface layers, the results of extensive tests performed with deflection-based and seismic-based nondestructive devices are presented. The technologies in this field are briefly overviewed and obtained results are compared from various aspects.

Keywords: pavement; delamination; deflection-based methods; seismic methods

Information

Received:

12.04.2020

Received in revised:

13.05.2020

Accepted:

30.06.2020

1. Introduction

Hot mix asphalt pavements which are paved on runways and major highways are composed of several different layers. Transferring the load uniformly through the pavement system is expected from a fully-bonded pavement structure [1-5]. If a complete bond between the layers cannot be obtained, the bearing capacity of pavement decreases and, in some cases, slippage may occur.

One of the consequences of poor bonding is the formation of delamination. Undetected delamination leads to the deterioration of HMA overlays on the surface of the roadway [6].

Debonding or delamination can occur in three modes [7]. delamination between two HMA layers, debonding between asphalt overlay and rigid pavement (PCC) slab, and debonding between asphalt layer and base course.

These debonding or delamination types effect the both structural and functional capacity of pavements. The most important delamination form is the shallow delamination of between two asphalt layers and debonding of thin asphalt overlays over rigid concrete slabs. In order to increase the bonding at the interfaces between layers of pavement, tack coat can be implemented. Thus, pavement functions as a monolithic system under traffic and environmental effects. Previous studies performed on the strength of HMA interface have demonstrated that being strong of tack coat bonding between the layers of a pavement has high level of importance in terms of transfer the radial tensile and shear stresses into the whole structure of pavement. On the other hand, existing of unbound layers or insufficient bonding of layers decreases the bearing capacity of pavement and may cause slippage. Insufficient bonding may also cause to concentrating of the tensile stresses at the bottom of the wearing course [8-10].

The assessment of the debonding or potential of delamination is typically carried out with bond strength

*Corresponding author: selcanertem@gmail.com (F. S. Ozen), +90 505 3367722

tests [11, 12]. The effectiveness of the tack coat varies depending on the aggregate gradation. Tack coats are generally more effective in fine-grained mixes than coarse-grained ones. The bond strength is also sensitive to the temperature of the tack coat during the test.

Study about the interface adhesion properties of hot mix asphalt layers based on the laboratory shear tests was conducted by Uzan et al [13]. Asphalt concrete specimens with different tack coats were tested at ambient temperature and elevated temperature under different normal stresses.

For determining the debonding or potential delamination occurred during or shortly after construction, using of a practical nondestructive testing (NDT) tool which is capable of detecting them is preferred. The impulse response (IR) method was used for determining the bonding condition within asphalt layers under controlled laboratory conditions [14]. In order to compare the responses from bonded, debonded and partially bonded interface conditions, thicknesses of different HMA surface layers were considered. As well as the transfer function between the applied load and measured deflection time histories (quantitative measure), the characteristics of the response (qualitative measure) were used to differentiate the different interface conditions, too. Cores taken from the tested locations showed that there is a good agreement between the interface condition predicted by using IR method and the interface shear strength obtained from laboratory test results.

Seismic Pavement Analyzer (SPA) and Portable Seismic Pavement Analyzer (PSPA) testing devices were firstly developed by Nazarian et al [15]. After this important progress, the SPA technology was mounted in a portable hand-held testing device called as the modulus of the surface layers can rapidly be measured by using the PSPA in the field conditions. The operating procedure of the PSPA is based on generating and detecting stress waves in a layer. Due to the sensitivity to thin near-surface layers, the PSPA can be used for the detection of the delamination within asphalt pavement layers.

There exists a lot of research regarding the usage of the Falling Weight Deflectometer (FWD) to detect the delamination between interfaces of asphalt pavement layers. According to the past experience, complicated results were seen in the detecting of delamination with FWD [16]. In the large part of the literature, a decrease seen in stiffness of bituminous or unexpected decline of backcalculated HMA modules are pointed out as an indication of debonding [10, 16-22].

In this paper, in detection of delamination and debonding, the results obtained from the evaluation of the weaknesses and strengths of the FWD and PSPA are presented. The two technologies are briefly overviewed and their results are compared. More information and

the details about other NDT techniques that can potentially be used for detection of debonding can be found in Celaya et al [23].

2. NDT Methods

As well as maximum deflections up to nine and the maximum load applied, the FWD readily provides deflection values for detailed analysis (Figure 1). In the study, 4.45 kN loading and the deflections measured by seven sensors (placed at 30.5 equally cm intervals) were used. After a comprehensive study, the most reliable analysis of debonding by using deflection data obtained from FWD was found to be provided by either the deflection under the load or the modulus of the asphalt layer after backcalculation process [23, 24].



Figure 1. Falling Weight Deflectometer on Small Scale Study; (A) FWD, (B) Loading Plate

Unlike the FWD that measures the response of the pavement system, working principle of the PSPA based on the wave propagation in layered systems. Specifically, the Ultrasonic Surface Wave (USW) method [25] implemented to the PSPA was used. The USW method is a seismic-based method. The stripping in HMA has been detected successfully by using this method [26]. The PSPA (see Figure 2), consists of two ultrasonic transducers and a source packaged into a hand-portable system to perform the USW tests [27]. In order to predict an average modulus and the variation in modulus based on depth, the outputs of the two transducers are subjected to signal processing and spectral analysis procedures.

3. Case Study

Ten different asphalt pavement sections were constructed specifically for the study as seen in Figure 3. Each section was 2.7 m long by 3 m wide. During the construction, three transition zones were constructed to minimize the variability of the asphalt mixture. The pavement cross-section for all sections consisted of a prepared sandy silt subgrade and about 200 mm thickness of asphalt layer placed in three lifts. The bottom lift consisted of about 75 mm of a coarse (P-403 mix as per US Federal Aviation Administration Standards for Specifying Construction of Airports) mix and the middle lift 63 mm of a fine (P-401) mix. The top lift (63 mm thick) of Sections 1 to 5 is formed of a coarse P-403 mix and a fine P-401 mix forms the top lift of Sections 6 to 10.

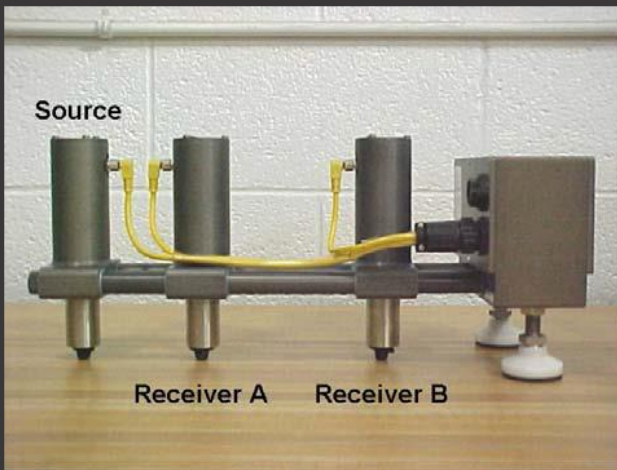


Figure 2. Portable Seismic Pavement Analyzer

Test locations are depicted in Figure 4. A 1.2 m by 3 m area for each section was intentionally debonded. Besides that, smaller debonded areas were constructed to perform the testing the detectability threshold of the methods. The effect of temperature on the test methods was evaluated by conducting tests in “cool” early spring temperatures (range of 15°C to 29°C) and “hot” summer temperatures (range of 24°C to 49°C).

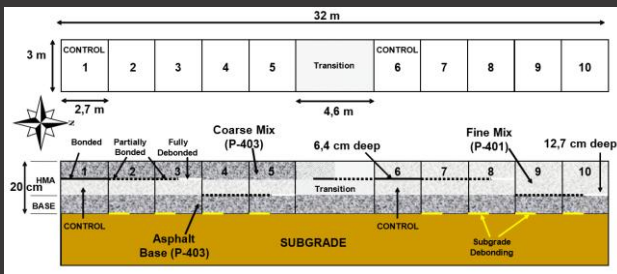


Figure 3. Schematic of small scale section

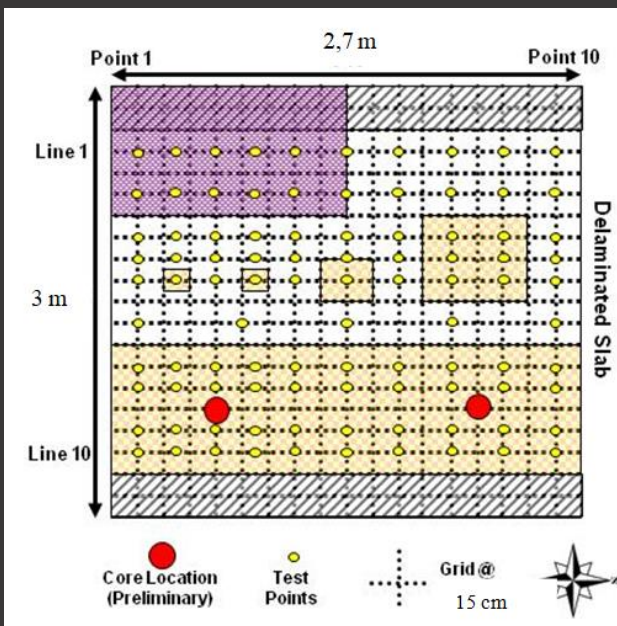


Figure 4. Location of test points

Several debonding agents were used to simulate different levels of debonding. Bond strengths were measured in the laboratory by conducting direct shear tests on

prepared specimens as discussed by Celaya et al [23]. Clay slurry, talcum powder, grease, and thin paper soaked in motor oil were considered as debonding agents. A tack coat in compliance with Item P-603 of FAA Standards for Specifying Construction of Airports [28] at a rate of 0.7 lit/m² was used as the control bonding agent. While the highest bond strength was associated with the tack coat, the lowest one was associated with a thin paper soaked in motor oil. Based on the shear strength results, it was considered that sections constructed with the tack coat are fully-bonded. Sections with the clay slurry, talcum powder and grease were considered as partially-debonded, and those with oily paper as fully-debonded. A severely debonded area was created in the transition area by laying a piece of thick corrugated cardboard and a thick layer of clay slurry.

Shallow and deep debonding was simulated by placing the debonding agent between the top two lifts (at a depth of 63 mm) and bottom two lifts (a depth of 125 mm), respectively. The characteristics of all sections are fully described in Celaya et al [7] and Ertem [24].

In this study, at that time, testing location temperature greatly affected the outcomes of the methods. Therefore, a lot of tests were performed were tested repeatedly at different times and different structural points corresponding to different temperature values. Then, relationships which are specific to site were developed for each method to be used.

3.1. Falling Weight Deflectometer (FWD)

In the study, we used the FWD. An impact loading system and seven geophones were mounted on the device to determine vertical surface deflections. Geophones were firstly placed right underneath the load and then at 300 mm intervals, respectively. Measurements were taken at selected locations of each section with the loading device which has a 300 mm diameter load plate and about 27 kN equivalent load. A seating drop was firstly applied for each test, followed by three additional drops. The average vertical displacement of the last three drops was measured with each geophone which was operated for every test location.

Deflections measured for the study the at the site locations are shown in Figure 5. Deflections measured with Geophones 1 and 2 (labeled as SD1 and SD2) are noticeably greater at the severely debonded location. For the others, small differences were measured between intact and debonded deflections.

25 points on each section (at 40 points on the transition zone) were chosen for the FWD test applications. After temperature adjustment, the resulting values were compared using color-coding in Figures 6. The average and standard deviation of each control section (1 and 6) were used as reference. One half and one standard

deviation were used to evaluate the results (deflections measured above the average minus one-half standard deviation are colored as green, which ones between average minus one-half and average minus one standard deviation are colored as yellow and which ones less than average minus one standard deviation are colored as red).

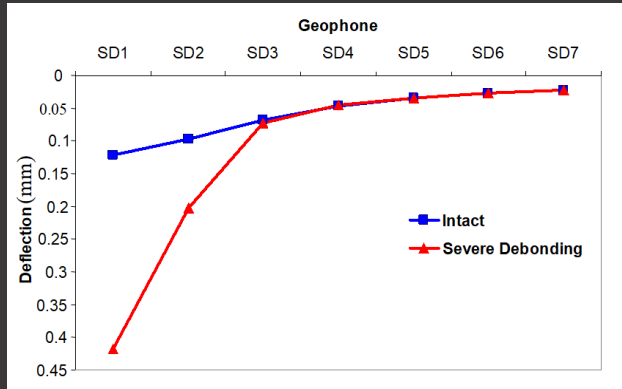


Figure 5. Typical deflections basins from FWD Tests

Since the FWD deflections are strongly affected by the subgrade modulus value, the next step was to test the variation in the asphalt layer modulus value as a means of detecting debonded sites. The asphalt layer moduli were backcalculated by using MODULUS 6.0 software [29]. A two-layered analysis that considered the entire asphalt layer thickness (200 mm) as one layer over a subgrade was used. The temperature adjusted modulus contour maps are shown in Figure 7.

3.2. Ultrasonic Surface Wave (USW) Method

USW tests were conducted by using PSPA device. For an intact and a severely debonded area, examples of the typical voltage outputs of the three PSPA sensors as seen by the operator in the field are shown in Figure 8. The time records obtained from the two receivers (the black and green traces) are considerably different from the two tests. The pulses are wider for the debonded record, and when the minima of the records between intact and damaged areas were compared, it can be seen that the intact areas are closer to one another.

The USW analysis page seen by the operator in the field is shown in Figure 9. The top graphs indicate the variation in modulus depending on wavelength (called dispersion curves). The dispersion curve for the intact area is fairly uniform; whereas for the damaged point, there is a sharp decrease in the modulus below a wavelength of 63 mm (the location of the damage). The vertical red lines in the graphs indicate the average moduli of the asphalt layer from close to surface (25 mm to 200 mm nominal thickness of the layer). As reflected in the left-hand side of the two graphs, these average moduli values are about 10 GPa for the intact areas and 7.8 GPa for the damaged areas.

	S1, Intact					S2, Shallow Partial					S3, Shallow Partial/Full					S4, Deep Partial					S5, Deep Partial/Full					TRANSITION			
	P1	P2	P3	P4	P5	P1	P2	P3	P4	P5	P1	P2	P3	P4	P5	P1	P2	P3	P4	P5	P1	P2	P3	P4	P5	P1	P2	P3	P4
N/A																													
Line 1	7.3	6.6	6.1	5.8	5.6	6.1	6.5	6.4	6.4	7.0	7.4	7.5	7.3	6.7	6.5	6.8	7.0	6.6	5.7	5.2	5.1	5.1	5.2	6.1	6.2	6.2	6.3	6.5	6.9
Line 2	8.0	7.2	6.3	6.1	6.1	6.1	6.3	6.5	6.8	6.6	6.3	6.7	8.1	7.6	7.7	6.9	7.2	7.7	6.4	5.3	5.1	5.3	5.7	7.1	6.6	6.5	6.6	9.0	9.1
Line 3	9.1	8.8	8.3	8.1	7.8	8.2	8.3	8.1	8.2	8.6	9.7	10.6	10.7	####	12.1	10.3	9.7	8.3	7.6	6.9	7.3	7.9	7.3	7.3	6.9	6.2	7.3	19.9	18.8
Line 4	10.8	10.7	9.6	9.5	9.1	8.6	9.6	9.8	9.2	9.8	10.8	11.3	12.2	####	12.8	10.9	10.0	8.3	7.9	7.2	7.7	8.3	7.2	7.7	7.4	6.9	7.7	18.7	16.8
Line 5	13.7	13.4	12.7	12.0	11.2	12.0	12.6	12.4	####	12.7	14.0	15.4	15.0	####	18.4	15.3	14.0	9.9	9.1	8.5	9.4	9.8	8.5	8.6	9.0	8.7	9.4	19.5	18.3
N/A																													

Sections 1 – 5

	TRANSITION				S6, Intact					S7, Shallow Partial					S8, Shallow Partial/Full					S9, Deep Partial					S10, Deep Partial/Full				
	P5	P6	P7	P8	P1	P2	P3	P4	P5	P1	P2	P3	P4	P5	P1	P2	P3	P4	P5	P1	P2	P3	P4	P5	P1	P2	P3	P4	P5
N/A																													
Line 1	8.0	8.4	8.4	8.2	7.4	7.5	8.0	8.0	8.1	7.4	7.5	7.3	7.2	7.1	7.0	7.2	7.5	7.3	6.4	5.6	5.3	4.8	5.1	4.9	5.0	5.1	4.8	4.5	4.6
Line 2	7.5	8.4	7.5	7.6	7.3	7.5	7.8	7.5	8.2	8.1	8.0	8.1	8.4	8.1	7.5	7.5	7.7	8.6	7.8	6.3	6.2	5.5	5.7	5.6	5.4	5.1	5.0	4.7	4.5
Line 3	8.3	8.0	8.0	8.2	8.1	8.5	9.0	9.0	8.8	9.3	9.4	9.1	8.3	8.4	8.9	9.5	9.8	####	10.7	8.2	7.7	7.1	6.9	6.7	7.4	7.7	7.2	6.9	6.4
Line 4	9.0	8.5	8.5	8.9	8.9	9.8	9.9	9.5	9.1	9.6	9.4	9.1	8.5	8.5	9.2	10.3	10.3	####	10.7	7.4	7.7	7.1	6.9	6.7	7.2	7.4	6.9	6.7	5.9
Line 5	9.9	9.7	9.6	9.8	10.5	11.4	11.4	11.2	10.4	10.4	10.7	10.0	9.7	9.8	11.2	12.5	13.5	####	14.0	10.1	9.0	8.8	8.2	7.9	8.2	9.6	9.3	8.5	7.4
N/A																													

Sections 6 – 10

Figure 6. Temperature-Adjusted Contour Maps of FWD Deflection



Figure 7. Temperature-Adjusted Contour Maps of FWD Moduli in Cool Weather based on Revised Statistical Criteria

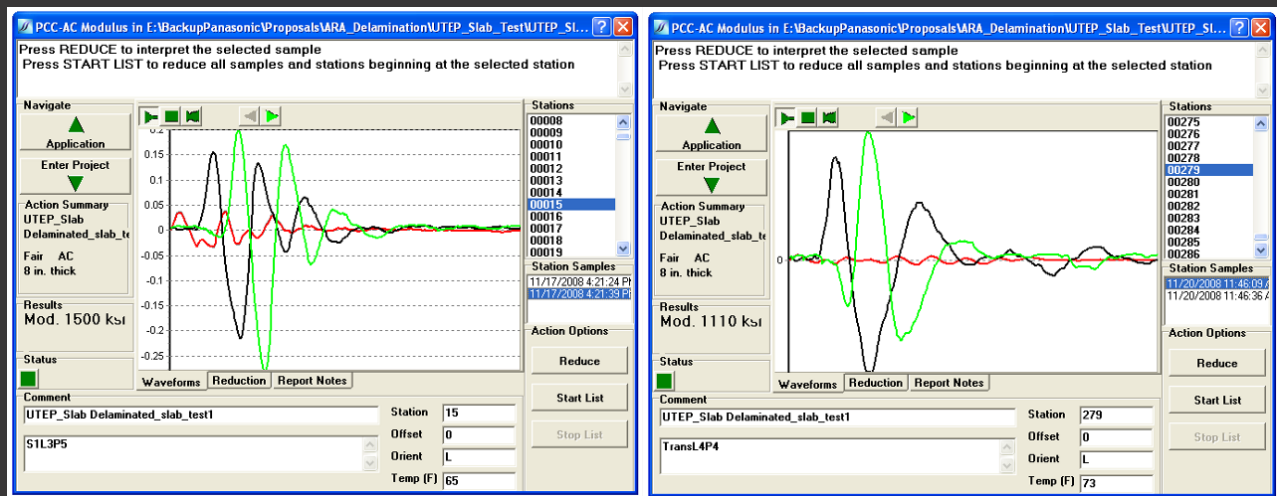


Figure 8. Time Records Results with PSPA on Small Scale Study: Intact (Left), Severe Debonding (Right)

The variations in the average moduli along the ten sections after temperature adjustment are compared in Figure 10 by using the color-coding convention as described for FWD. The contour plot of the average moduli of the top lift (top 63 mm) for the ten sections tested in cool weather is shown in Figure 11. It is observed that there are reduced moduli for particularly Sections 3 and 8 (shallow and full debonding). Sections with the shallow and partial debonding also showed some reduction in the moduli. This pattern indicates that when the two adjacent layers are not bonded, quality of the asphalt layer (in terms of the stiffness) may be endangered.

Detailed dispersion curves for Line 1 (intact) and Line 10 (severely debonded) along the ten sections are presented in Figure 12. The depths and the extent of the debonding areas are also depicted in the figures. Here, solid lines indicate the full debonding and the dashed lines mean partial debonding. It is seen that the reductions in the modulus can be observed in most debonded sections at or below the depths of defects, at least in identifying the fully debonded areas, the usefulness of the USW method is validated. One complicating (but perhaps beneficial) aspect of the dispersion curve is that in a dispersion curve, a low-quality but bonded lift may exhibit the same patterns with a partially debonded interface.

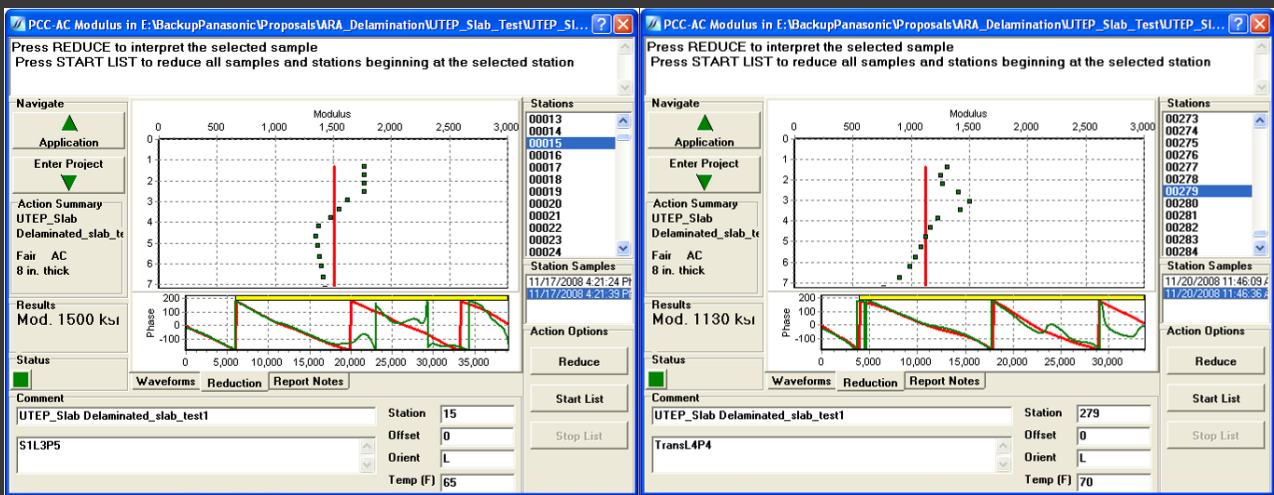
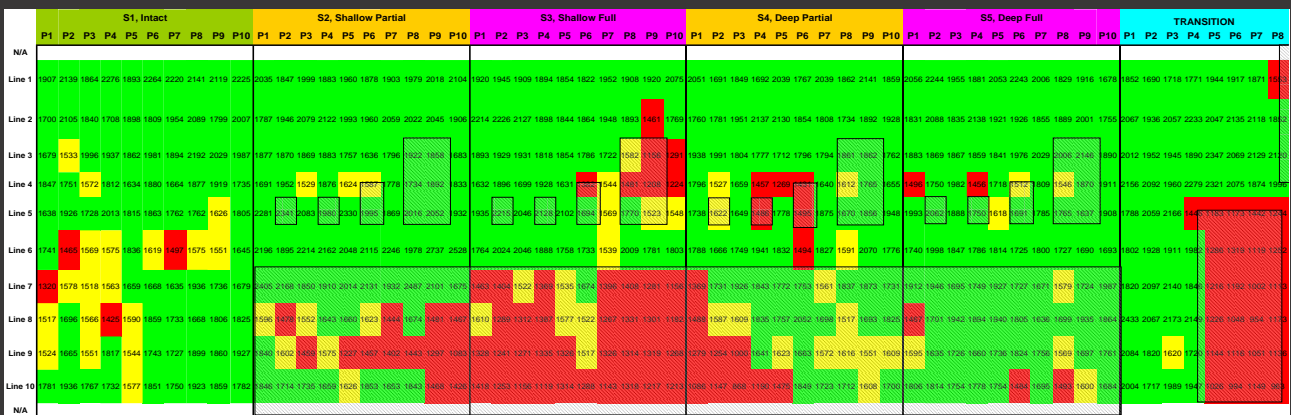


Figure 9. Dispersion Curve Results with PSPA on Small Scale Study: Intact (Left), Severe Debonding (Right)



Sections 1 to 5



Sections 6 to 10

Figure 10. Temperature-Adjusted Contour Maps of PSPA Modulus

4. Conclusions

The USW method and the FWD technique were extensively evaluated on a control pavement section which is specifically constructed by using different HMA mixes at different depths and have various levels of debonding. Both NDT methods detected a severely debonded section well. Based on the outcomes of the study, the following interpretations can be made:

- In general, both methods were capable to locate damaged areas, with a high probability of success.
- Both methods detected the shallow (less than 3 in. (75 mm) deep) and severely debonded areas with reasonable certainty.
- The USW method as implemented in the PSPA could detect 53% of the debonded areas. PSPA could detect the best the shallow debonding (both partial and full).
- The FWD could detect about 46% of the debonded areas based on the backcalculation of the modulus of the HMA layer.
- The temperature adjustment is required for both FWD and USW methods to get success. For complex pavement sections, the FWD has slightly limited effectiveness.

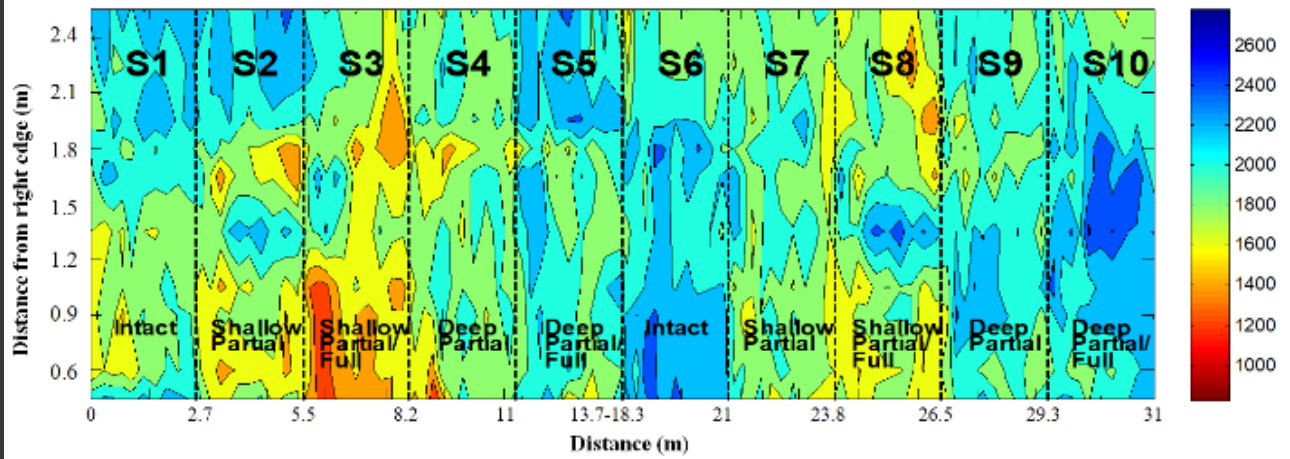


Figure 11. Modulus Contour Plot of Top 6.4 cm

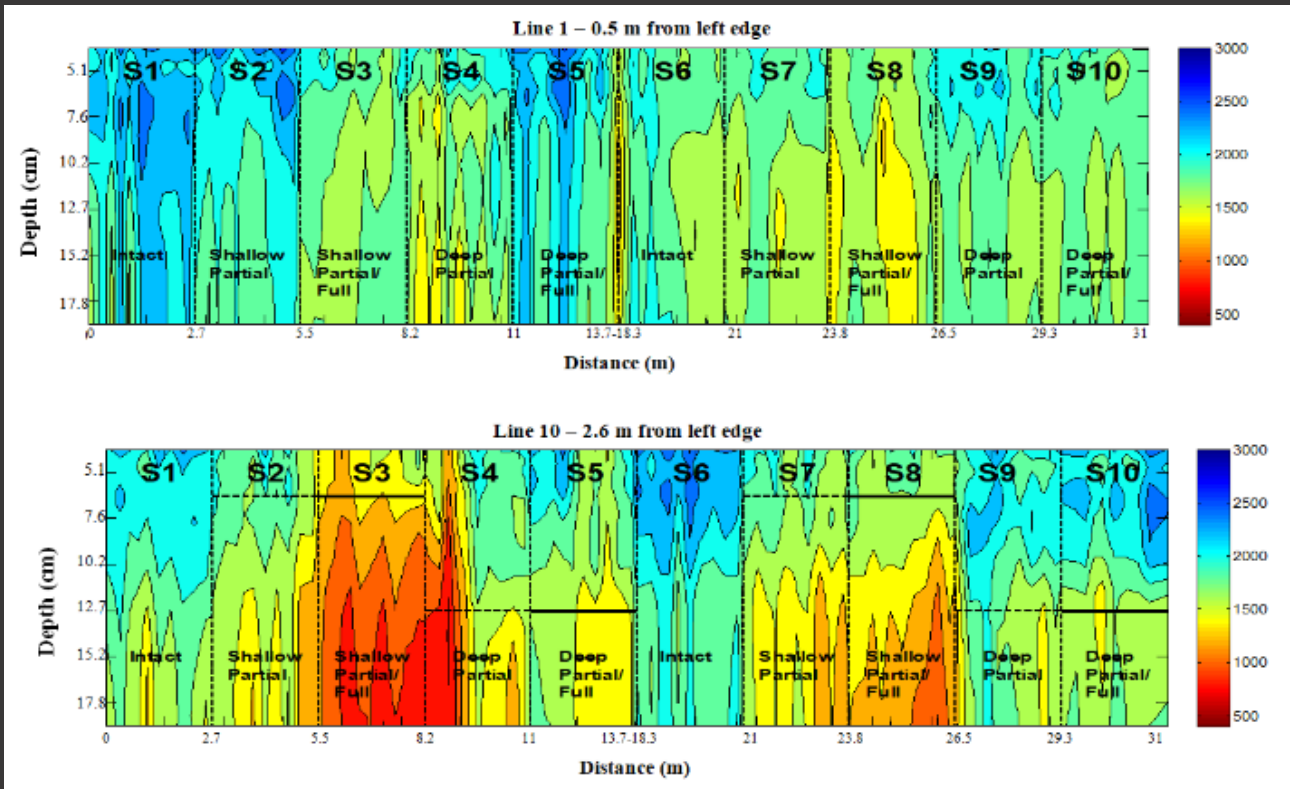


Figure 12. Dispersion Curve Contour Plots for Lines 1 and 10

Declaration of Interest Statement

The authors declare that they have no known competing financial interests or personal relationships that could have appeared to influence the work reported in this paper.

Author Contribution Statement

F. S. Ozen: Conceptualization, Formal analysis, Investigation, Methodology, Project Administration, Resources, Software, Supervision, Validation, Visualization, Draft writing, Review&Editing – **M. Celaya:** Conceptualization, Formal analysis, Investigation, Methodology, Project Administration, Resources, Software, Supervision, Validation, Visualization, Draft

writing, Review&Editing – **S. Nazarian:** Conceptualization, Formal analysis, Investigation, Methodology, Project Administration, Resources, Software, Supervision, Validation, Visualization, Draft writing, Review&Editing – **M. Saltan:** Conceptualization, Formal analysis, Investigation, Methodology, Project Administration, Resources, Software, Supervision, Validation, Visualization, Draft writing, Review&Editing

Acknowledgements

The authors wish to gratefully acknowledge the support of the Airfield Asphalt Pavement Technology Program (AAPTTP).

References

- [1] Mehta, Y., & Siraj, N. (2007). Effect of Stiffness Ratio on Slippage Cracking Due to Interlayer Bonding Failure in Hot Mix Asphalt Pavement. In 2007 Mid-Continent Transportation Research Symposium Department of Transportation Iowa State University, AmesMidwest Transportation Consortium.
- [2] Petit, C., Chabot, A., Destrée, A., & Raab, C. (2018). Interface debonding behavior. In *Mechanisms of cracking and debonding in asphalt and composite pavements* (pp. 103-153). Springer, Cham. https://doi.org/10.1007/978-3-319-76849-6_3
- [3] Tebaldi, G., Apeagyei, A., Jelagin, D., & Falchetto, A. C. (2018). Advanced Measurement Systems For Crack Characterization. In *Mechanisms of Cracking and Debonding in Asphalt and Composite Pavements* (pp. 155-227). Springer, Cham. https://doi.org/10.1007/978-3-319-76849-6_4
- [4] Mousa, M., Elseifi, M. A., Elbagalati, O., & Mohammad, L. N. (2019). Evaluation of interface bonding conditions based on non-destructing testing deflection measurements. *Road Materials and Pavement Design*, 20(3), 554-571. <https://doi.org/10.1080/14680629.2017.1400995>
- [5] Le, M. T., Nguyen, Q. H., & Nguyen, M. L. (2020). Numerical and Experimental Investigations of Asphalt Pavement Behaviour, Taking into Account Interface Bonding Conditions. *Infrastructures*, 5(2), 21. <https://doi.org/10.3390/infrastructures5020021>
- [6] www.usroads.com Road Management & Engineering. www.usroads.com/journals/rmj/9704/rm970403
- [7] Celaya, M., Mejia, D., Ertem, S., Nazarian, S., Rao, C., Von Quintus, H., & Shokouhi, P. (2010). Evaluation of NDT technologies to assess presence and extent of delamination of HMA airfield pavements. Final Rep., Airfield Asphalt Pavement Technology Program, Federal Aviation Administration.
- [8] Mohammad, L. N., Wu, Z., & Raqib, A. (2005). Investigation of the behavior of asphalt tack interface layer, Louisiana Transportation Research Center, FHWA/LA. 04/394.
- [9] Li, M., Anderson, N. L., Sneed, L. H., & Kang, X. (2016). An assessment of concrete over asphalt pavement using both the ultrasonic surface wave and impact echo techniques. *Journal of Environmental and Engineering Geophysics*, 21(4), 137-149. <https://doi.org/10.2113/JEEG21.4.137>
- [10] Li, M., Wang, H., Xu, G., & Xie, P. (2017). Finite element modeling and parametric analysis of viscoelastic and nonlinear pavement responses under dynamic FWD loading. *Construction and Building Materials*, 141, 23-35. <https://doi.org/10.1016/j.conbuildmat.2017.02.096>
- [11] West, R. C., Moore, J. R., & Zhang, J. (2006). Evaluating tack coat applications and the bond strength between pavement layers. In *Airfield and Highway Pavement: Meeting Today's Challenges with Emerging Technologies* (pp. 578-588). [https://doi.org/10.1061/40838\(191\)49](https://doi.org/10.1061/40838(191)49)
- [12] Gregory, A. S., Galr, C. P., James, A. M., Patrik, B. U., & Howard, L. M. (2002). Preliminary Investigation of a Test Method to Evaluate Bond Strength of Bituminous Tack Coats. Research Report, Florida DOT, FL/DOT/SMO/02-459.
- [13] Uzan, J., Livneh, M., & Eshed, Y. (1978). Investigation of adhesion properties between asphaltic-concrete layers. In *Association of Asphalt Paving Technologists Proc* (Vol. 47).
- [14] Kruntcheva, M. R., Collop, A. C., & Thom, N. H. (2004). Feasibility of assessing bond condition of asphalt concrete layers with dynamic nondestructive testing. *Journal of transportation engineering*, 130(4), 510-518. [https://doi.org/10.1061/\(ASCE\)0733-947X\(2004\)130:4\(510\)](https://doi.org/10.1061/(ASCE)0733-947X(2004)130:4(510))
- [15] Nazarian, S., Baker, M. R., & Crain, K. (1993). Developing and testing of a seismic pavement analyzer. Technical Report SHRP-H, 375.
- [16] Mejia, D., Celaya, M., Iyer, S., Rao, C., Shokouhi, P., & Nazarian, S. (2008). A work plan toward evaluation of technologies to assess presence and extent of delamination of HMA airfield pavements. Research Project, 06-04.
- [17] Hammons, M. I., Von Quintus, H., Geary, G. M., Wu, P. Y., & Jared, D. M. (2006). Detection of stripping in hot-mix asphalt. *Transportation research record*, 1949(1), 20-31. <https://doi.org/10.1177/0361198106194900103>
- [18] Sangiorgi, C., Collop, A., & Thom, N. H. (2003). A non-destructive impulse hammer for evaluating the bond between asphalt layers in a road pavement, In: *International Symposium (NDTCE 2003) of Non-Destructive Testing in Civil Engineering*, Berlin, Germany.
- [19] Gomba, S. M. (2004). Evaluation of interlayer bonding in hot mix asphalt pavements, MS thesis, Rowan University, Glassboro, N.J.
- [20] Al Hakim, B., Armitage, R., & Thom, N. H. (1998). Pavement assessment including bonding condition: case studies. In *Proceedings, 5th International Conference on Bearing Capacity of Roads and Airfields*, University of Trondheim, Trondheim, Norway (Vol. 1, pp. 439-448).
- [21] Nguyen, A. D. (2016). Nondestructive evaluation of bonding condition of asphalt pavement based on measured deformation of the road, *Transportation Research Board*, No. 16-0211.
- [22] Cickovic, M. (2017). Non-destructive testing of layer bonding with the falling weight deflectometer (FWD). In *AAPA International Flexible Pavements Conference*, 17th, 2017, Melbourne, Victoria, Australia.
- [23] Celaya, M., Mejia, D., Ertem, S., Nazarian, S., Rao, C., Von Quintus, H., & Shokouhi, P. (2009). Evaluation of NDT technologies to assess presence and extent of

- delamination of HMA airfield pavements: Verification study. AATP Report for Project, 06-04.
- [24] Ertem, F.S. (2011). Determination of the Discontinuity of Highway Flexible Pavements Layers by Using Nondestructive Seismic Methods, PhD Thesis, Suleyman Demirel University, Isparta, Turkey.
- [25] Baker, M. R., Crain, K., & Nazarian, S. (1995). Determination of Pavement Thickness with a New Ultrasonic Device, Research Report 1966-1, Center for Highway Materials Research, The University of Texas at El Paso, El Paso, TX, 53 p.
- [26] Hammons, M. I., Von Quintus, H., Maser, K., & Nazarian, S. (2005). Detection of stripping in hot mix asphalt., Applied Research Associates Project Number 16355, prepared for: Office of Materials and Research, Georgia Department of Transportation, 2005.
- [27] Nazarian, S., Yuan, D., Smith, K., Ansari, F., & Gonzalez, C. (2006). Acceptance criteria of airfield concrete pavement using seismic and maturity concepts. Innovative Pavement Research Foundation, Airport Concrete Pavement Technology Program. Report IPRF-01-G-002-02-2.
- [28] Standards for Specifying Construction of Airports. Advisory Circular 150/5370-10E. U.S. Department of Transportation Federal Aviation Administration, 2009.
- [29] Liu, W., & Scullion, T. (2001). MODULUS 6.0 for windows: User's manual (No. FHWA/TX-05/0-1869-2). Texas Transportation Institute, Texas A & M University System.